

Laser-induced fluorescence line narrowing in Sm^{2+} -doped fluoride glass

Masanori Tanaka and Takashi Kushida

Department of Physics, Osaka University, Toyonaka, Osaka 560, Japan

(Received 27 September 1993)

Fluorescence line-narrowing experiments have been made for the Sm^{2+} ion in fluoride glass at 77 K under cw dye-laser excitation at various energies within the inhomogeneously broadened 7F_0 - 5D_0 and 7F_0 - 5D_1 absorption lines. The energies of the three Stark levels of the 7F_1 and 5D_1 manifolds have been obtained as a function of the 5D_0 - 7F_0 energy separation. From the analysis of this result, it has been found that the site-to-site variations of the energies of these Stark levels can be explained well only by taking into account the J -mixing effect. The low-energy levels of the $4f^55d$ configuration lie in the vicinity of the 5D_J states in this material. However, no effect of the crystal-field mixing of the $4f^55d$ states on the inhomogeneous distribution of the energies of the 7F_1 and 5D_1 states has been observed. The origin of the unusually intense 5D_0 - 7F_0 transition in Sm^{2+} is also discussed.

I. INTRODUCTION

So far, the laser-induced-fluorescence line-narrowing method has been employed for the investigation of various crystals and glassy systems which contain paramagnetic ions and dye molecules, and has provided useful information about the local structure around these centers, vibrational modes of the host matrices, and so on.¹⁻²¹ In the $4f^N$ - $4f^N$ (f - f) transition of trivalent rare-earth ions, the fluorescence line-narrowing (FLN) effect is observed rather easily, because the homogeneous widths of the f - f transitions are often much narrower than the inhomogeneous widths, especially at low temperatures. This is because of the weakness of the coupling between the $4f$ electrons and the host material, which results from the shielding of the $4f$ electrons from the surroundings by the outer $5s^25p^6$ electrons. Furthermore, since the wave functions of the $4f^N$ free-ion states of the trivalent rare-earth ions are well known, the symmetry of the ion site and strength of the local field acting on the ion can be determined relatively easily from the numbers and magnitudes of the splittings of the J manifolds. For these reasons, trivalent rare-earth ions have often been employed in the FLN experiments as useful probes of the local environment of these ions.

In particular, the FLN spectra of the 5D_0 - ${}^7F_{0,1,2}$ transitions of the Eu^{3+} ion have been studied for a number of inorganic glasses, and have yielded valuable information on the local field acting on the Eu^{3+} ion.^{4-13,15-18} This is because the initial state of these transitions, 5D_0 , is a nondegenerate state, and the final states have J values of small integers, so that the optical spectra of these transitions are simple and their analysis is fairly easy. Brecher and Riseberg^{7,8} analyzed these FLN spectra of the Eu^{3+} ion in oxide and fluoride glasses and proposed geometric models for the first coordination sphere of the Eu^{3+} ion. On the other hand, Brawer and Weber^{12,13} simulated glass structure with Monte Carlo and molecular-dynamics calculations. They reproduced well the observed FLN spectra of Eu^{3+} doped into the fluoroberyllate glass by employing the point-charge model and a

simulated glass structure for the Eu^{3+} and the surrounding ions. Nishimura and Kushida^{15,16} made detailed studies of the FLN spectra of Eu^{3+} in calcium metaphosphate glass and determined the inhomogeneous distribution of the crystal-field parameter values. They further identified the 5D_0 - 7F_0 transition mechanism and clarified the origin of the asymmetric spectral shape of the inhomogeneously broadened 5D_0 - 7F_0 line.

Recently, the persistent spectral hole-burning phenomenon has been observed at room temperature for the f - f transitions of the Sm^{2+} ion doped into mixed crystals,^{22,23} and fluoride glasses.^{24,25} Glass is considered to be more favorable as the host material for high-density optical memory devices than crystalline matrices, because the inhomogeneous width of the f - f transition is much broader, there is large freedom in size and shape in production, and also it is less expensive. However, the optical properties of Sm^{2+} -doped glass are not known well yet.

The structure of the electronic energy levels is almost the same for the Eu^{3+} and isoelectronic Sm^{2+} ions,²⁶ although the energy separations between the $4f^6$ and $4f^55d$ states are much different. Therefore, a FLN experiment is considered to be effective also for Sm^{2+} -doped glasses. In this paper, we report a FLN measurement in a Sm^{2+} -doped fluoride glass. As far as we know, this is the first FLN experiment in a Sm^{2+} -doped material. From comparison of the observed fluorescence properties with those reported in several kinds of glasses doped with Eu^{3+} , we can obtain information on the local environment around the Sm^{2+} ion. In our sample the low-energy tail of the absorption band due to the $4f^6$ - $4f^55d$ (f - d) transition lies in such a low-energy region as to overlap with the 7F_0 - 5D_J transitions. We also examine the possibility that this fact affects the properties of the FLN spectra.

II. EXPERIMENTAL RESULTS AND DISCUSSION

The fluoride glass sample was provided by Izumitani's laboratory of the Hoya Corporation. The sample was a

(28.2) AlF_3 - and (12.2) HfF_4 -based glass which contains (8.3) YF_3 , (3.5) MgF_2 , (18.3) CaF_2 , (13.1) SrF_2 , (12.6) BaF_2 , and (3.8) NaF as all concentrations expressed as modifiers (mole %).²⁷ The trivalent samarium ion added in the form of SmF_3 (~3 mole %) was partly converted to the divalent state in a reducing atmosphere. Though the Sm^{2+} ions are considered to be very few compared to Sm^{3+} , the ratio of these ions is not well known.²⁵

A. Absorption and ordinary fluorescence spectra

The absorption spectrum of this sample in the 200–700-nm wavelength range was reported by Izumitani and Payne.²⁷ An intense, broad asymmetric band, which is peaked around 320 nm, is ascribed to the parity-allowed f - d transition of Sm^{2+} . On the other hand, the f - f transitions of Sm^{2+} and Sm^{3+} are not observed distinctly except for a sharp peak around 390 nm, which probably corresponds to the spin-allowed ${}^6H_{5/2}$ - 6P_J transition of Sm^{3+} . Figure 1 shows the fluorescence spectrum of our sample at 77 K under the excitation of all lines of an Ar^+ laser. In this case, the Sm^{3+} ion is considered to be excited into the 4G , 4F , and 4I states, while the Sm^{2+} ion is excited into the low-energy tail of the $4f^55d$ absorption band.

In Fig. 1, the five transitions in the lower-energy region, 5D_0 - 7F_J ($J=0,1,2,3,4$), are due to the Sm^{2+} ion, while the three transitions in the higher-energy region, ${}^4G_{5/2}$ - 6H_J ($J=\frac{5}{2}, \frac{7}{2}, \frac{9}{2}$), are ascribed to the Sm^{3+} ion. The FLN effect is not important in this case, and the spectra are considered to be inhomogeneously broadened. The fluorescence lines of the Sm^{2+} ion originating from the energy levels above the 5D_0 state are not observed. The spectral profiles of the transitions of the Sm^{3+} ion are very similar to those of the same ion in lanthanum aluminum silicate glass.¹¹

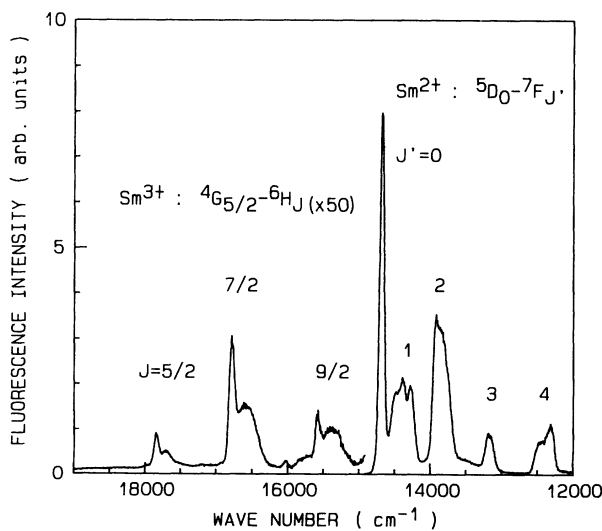


FIG. 1. Fluorescence spectrum of a Sm-doped fluoride glass sample at 77 K under excitation by all lines of an Ar^+ laser. Corrections have been made for the wavelength dependence of the transmittance of the monochromator and the sensitivity of the photodetector.

A remarkable temperature-quenching phenomenon is observed for the 5D_0 - 7F_J ($J=0,1,2,3,4$) fluorescence transitions in the range from 4 to 300 K under the excitation of all lines of an Ar^+ laser. It was found that the intensities of all the above transitions decrease at the same rate with increasing temperature. The sum of the above fluorescence intensities, which were calculated from the spectra measured by Kurita,²⁸ is plotted in Fig. 2 as a function of temperature. In our sample, the energy of the 5D_0 state of the Sm^{2+} ion is lower than those of the $4f^55d$ states, as is evident from the absorption spectrum measured by Izumitani and Payne.²⁷ In such a case, almost all the fluorescence of the Sm^{2+} ion is considered to be emitted after the ions excited into the $4f^55d$ state relax nonradiatively into the 5D_0 state, and therefore the vertical axis of Fig. 2 is proportional to the overall fluorescence quantum efficiency of the Sm^{2+} ion. In addition, the overall fluorescence quantum efficiency of the Sm^{2+} ion is expected to be expressed as²⁷

$$\eta = \eta_d \eta_f, \quad (1)$$

where η_d is the efficiency of the relaxation of the Sm^{2+} ion excited into the $4f^55d$ state to the 5D_0 state and η_f is the fluorescence efficiency of the ion in the 5D_0 state. From fitting of the temperature dependence of the lifetime of the 5D_0 state, Izumitani and Payne²⁷ found that η_f is expressed as

$$\eta_f = [1 + 15.1 \exp(-\Delta E/k_B T)]^{-1}, \quad (2)$$

with $\Delta E = 630 \text{ cm}^{-1}$, where k_B is Boltzmann's constant and T is the absolute temperature. This type of temperature dependence of the fluorescence efficiency is usually observed for broadband fluorescence in systems with strong electron-lattice coupling. However, it is rare that it is observed for the f - f transitions of a rare-earth ion.

When we employ the above relation (2) and also the following expression for η_d :

$$\eta_d = [1 + r \exp(-\Delta E'/k_B T)]^{-1}, \quad (3)$$

with $r = 6.2$ and $\Delta E' = 345 \text{ cm}^{-1}$, we can fit the experimental data well with Eq. (1), as shown by the solid line

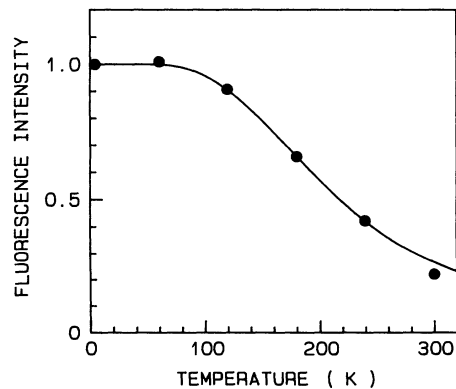


FIG. 2. Temperature dependence of the sum of the 5D_0 - 7F_J ($J=0,1,2,3,4$) fluorescence intensities of Sm^{2+} in fluoride glass. The solid line has been obtained using Eqs. (1)–(3).

in Fig. 2. Izumitani and Payne²⁷ explained the relation between the lifetime of the 5D_0 state and the overall fluorescence quantum efficiency η in three different kinds of fluoride glasses containing various concentrations of samarium, assuming that $\exp(-\Delta E'/k_B T)$ is directly proportional to $\exp(-\Delta E/k_B T)$ and accordingly $\Delta E'$ is equal to $\Delta E = 630 \text{ cm}^{-1}$. However, we could not fit our temperature-dependence data of the fluorescence intensity well with Eq. (1) by putting $\Delta E' = 630 \text{ cm}^{-1}$. In order to explain the temperature dependence of the lifetime of the 5D_0 state, the above authors proposed a model in which the Sm^{2+} ion in $4f^55d$ states and also in the 5D_0 state can relax nonradiatively into the 7F_J states through conduction-band-like states of the host glass. If we employ this model, $\Delta E'$ in Eq. (3) can be interpreted in terms of the activation energy for the transition from the $4f^55d$ states to the host conduction-band-like states. Further, r represents the ratio between the relaxation rate from the $4f^55d$ states to the 5D_J states and the frequency factor for the transition from the $4f^55d$ states to the host conduction-band-like states.

In the ${}^4G_{5/2}$ - ${}^6H_{5/2,7/2,9/2}$ lines of the Sm^{3+} ion, temperature quenching was not observed in the 4–300-K temperature range. The energy gap between the ${}^4G_{5/2}$ and the next lower ${}^6F_{11/2}$ state is as large as about 7000 cm^{-1} . On the other hand, from the energies of the vibrations that couple with the Eu^{3+} ion in several kinds of fluoride glasses,²⁹ those that couple with the Sm^{3+} ion in our sample, which probably are the vibrations of the bond between F^- and cations in the glass such as Sm^{3+} , Al^{3+} , and Hf^{4+} , are believed to have relatively small energies, below about 600 cm^{-1} . Therefore, the contribution of the multiphonon nonradiative process to the relaxation of the ${}^4G_{5/2}$ state is considered to be fairly small,^{30–32} and the above result is explained well.

Hereafter, we discuss only the spectroscopic properties of the Sm^{2+} ion in the fluoride glass.

B. The 5D_0 - 7F_0 transition mechanism

We notice in Fig. 1 that the 5D_0 - 7F_0 line is rather intense compared with other lines, which is also so for the Sm^{2+} ion doped into several crystals.³³ The 5D_0 - 7F_1 transition is due to the parity-allowed magnetic-dipole transition, so that its intensity is considered to be insensitive to the strength of the crystal field. Moreover, the squared transition matrix elements for this transition of the Eu^{3+} and Sm^{2+} ions are almost equal in magnitude, because the wave functions of Eu^{3+} and Sm^{2+} in a free-ion state are nearly the same.²⁶ We can, therefore, use the intensity of the 5D_0 - 7F_1 fluorescence of Eu^{3+} and Sm^{2+} as a standard. Table I shows the intensity ratio of the 5D_0 - 7F_0 transition to the 5D_0 - 7F_1 transition in the Sm^{2+} -doped fluoride glass and Eu^{3+} -doped oxide glasses. This intensity ratio in the Sm^{2+} -doped glass is much larger than those in the Eu^{3+} ion doped into oxide glasses.

The dominant mechanism of the 5D_0 - 7F_0 transition of the Eu^{3+} ion in oxide glasses has been identified as a borrowing of intensity by the J -mixing effect^{15–18} from the 5D_0 - 7F_2 transition, which is explained by the Judd-Ofelt

TABLE I. Intensity ratio of the 5D_0 - 7F_0 transition to the 5D_0 - 7F_1 transition in Sm^{2+} -doped fluoride glass and Eu^{3+} -doped oxide glasses.

Sample	$I({}^5D_0\text{-}{}^7F_0)/I({}^5D_0\text{-}{}^7F_1)$
Fluoride glass: Sm^{2+}	0.87 ± 0.10^a
$\text{Ca}(\text{PO}_3)_2:\text{Eu}^{3+}$ (24 mole %)	0.048^b
$80\text{GeO}_2 \cdot 20\text{Na}_2\text{O} \cdot 1\text{Eu}_2\text{O}_3$	0.086 ± 0.015^b
$70\text{SiO}_2 \cdot 30\text{Na}_2\text{O} \cdot 1\text{Eu}_2\text{O}_3$	0.057 ± 0.012^b

^aEstimated from the fluorescence spectrum of Fig. 1.

^bEstimated from the inhomogeneously broadened fluorescence spectrum by the excitation of the 365-nm line of a Hg lamp.

theory^{34,35} and the Wybourne-Downer theory noted below.^{36–38} In the case of the Sm^{2+} ion in fluoride glass, on the other hand, the 5D_0 - 7F_0 transition is too intense to be explained by the J -mixing effect. As for the 5D_0 - 7F_0 transition mechanism in this sample, the following two mechanisms are probable.

(1) The breakdown of the closure approximation employed for the high-lying odd-parity states^{17,18,39} which mix into the 5D_0 and 7F_0 states through the linear crystal-field term in the Judd-Ofelt theory. The 5D_0 - 7F_0 transition due to this mechanism is expressed by the following type of matrix element:

$$\frac{\langle 4f^6[{}^5D]_0|\mu|{}^7L_1 \rangle \langle {}^7L_1|V_c^{(1)}|4f^6[{}^7F]_0 \rangle}{E({}^7L_1) - E({}^7F_0)} \quad (4)$$

(2) The mechanism which was proposed by Wybourne³⁶ and subsequently developed by Downer and co-workers.^{37,38} This mechanism is characterized by the following type of matrix element:

$$\frac{\langle 4f^6{}^5D_0|\mu|{}^5L'_1 \rangle \langle {}^5L'_1|H_{so}|{}^7L_1 \rangle \langle {}^7L_1|V_c^{(1)}|4f^6{}^7F_0 \rangle}{[E({}^5L'_1) - E({}^7F_0)][E({}^7L_1) - E({}^7F_0)]} \quad (5)$$

Here, μ and H_{so} are the electric-dipole moment and the spin-orbit interaction, respectively, and $V_c^{(1)}$ is the linear term of the crystal-field potential. Further, the ${}^5L'_1$ and 7L_1 states are the high-lying states with odd parity, and $E(\dots)$ represents the energy of the state in the parentheses. In Eq. (4), $[\dots]$ denotes that the quantities in the square brackets are not good quantum numbers because of the strong spin-orbit interaction acting within the $4f^N$ configuration states, which relaxes the spin-selection rule in the above mechanism (1). In contrast with this, the spin-orbit interaction within the high-lying electron configuration states relaxes the spin-selection rule in the mechanism (2). In both mechanisms, the linear term of the crystal-field potential at the Sm^{2+} ion site is necessary. Our sample satisfies this condition, as mentioned later.

There exist two causes that explain the large difference in the 5D_0 - 7F_0 transition strength between the Eu^{3+} -doped oxide glasses and the Sm^{2+} -doped fluoride glass in Table I. One is the difference in the magnitude of the linear crystal-field component acting on the rare-earth ions. The other is the difference in the energy positions

of the high-lying odd-parity states in these materials. In both mechanisms (1) and (2), the lower energies of the high-lying odd-parity states lead to higher intensities of the 5D_0 - 7F_0 transition, because both mechanisms are based on a forced electric-dipole transition. Furthermore, the expression (4) includes only one energy denominator, while the expression (5) has two. Accordingly, the square of the absolute value of the transition matrix element due to mechanism (2) is much more sensitive than that due to mechanism (1) to the energy difference between the high-lying odd-parity states and the states concerned with the optical transition.

In the case of the Eu^{3+} ion in condensed matter, the energies of the charge-transfer states are usually much lower than those of the $4f^55d$ states.⁴⁰ Therefore, the charge-transfer states are more important than the $4f^55d$ states as intermediate states of the electric-dipole f - f transition in Eu^{3+} -doped materials.⁴¹ For example, the charge-transfer bands of the Eu^{3+} -doped oxide glasses, which are considered to be due to the transfer of one $2p$ electron of the nearby O^{2-} to the $4f$ orbital of the Eu^{3+} ion, lie about $40\,000\text{ cm}^{-1}$ above the ground state,⁴² and the energy separation between the 7F_0 - 5D_0 and the charge-transfer transition is about $23\,000\text{ cm}^{-1}$. On the other hand, the energy of the lowest $4f^55d$ state of the Sm^{2+} ion in the fluoride glass is so low as to overlap with the 5D_J states. This difference in the energies of the high-lying states may account for the large difference in the 5D_0 - 7F_0 transition intensity between the Eu^{3+} and Sm^{2+} glass samples in Table I.

On the other hand, the intensity ratio of the 5D_0 - 7F_2 transition to the 5D_0 - 7F_1 transition of Sm^{2+} in fluoride glass is smaller than those of the Eu^{3+} ion in oxide glasses. This may be explained by an interference effect among the transition matrix elements related to the linear and cubic crystal-field components which cause the former transition.³⁴⁻³⁸

C. FLN experiment under 7F_0 - 5D_0 excitation

Figure 3 shows the FLN spectra of our sample due to the 5D_0 - 7F_1 transitions at 77 K for various excitation energies within the 7F_0 - 5D_0 absorption line. In this measurement, a cw DCM dye laser was used as the excitation source. Because it is known that hole burning occurs in the 7F_0 - 5D_0 line,²⁴ the exciting laser intensity was reduced sufficiently so that the hole burning was negligible. In Fig. 3, an additional peak is observed at about $14\,700\text{ cm}^{-1}$ for excitation into the high-energy side of the 7F_0 - 5D_0 absorption line. This peak is probably ascribed to the fluorescence of the ions to which the excitation energy is transferred from the resonantly excited ions. The energy of this peak remains constant when the excitation energy is varied and is nearly coincident with the peak energy of the inhomogeneously broadened 5D_0 - 7F_0 fluorescence line in Fig. 1. These results are consistent with the above mechanism of excitation migration.

Figure 4 shows the energies of the three lines of the 5D_0 - 7F_1 transition as a function of the 7F_0 - 5D_0 excitation energy. Since this energy is identical with the 5D_0 - 7F_0 energy separation for the site-selected ion, the horizontal

axis of this figure is considered to be a measure of the strength of the crystal field acting on the Sm^{2+} ion. If we assume that the energy of the 5D_0 state is insensitive to the 5D_0 - 7F_0 energy separation, which can be proved theoretically to be a good approximation,^{15,16,18} the vertical axis of Fig. 4 corresponds to the energies of the three Stark levels of the 7F_1 manifold. In Fig. 4, the energies of the three 5D_0 - 7F_1 lines vary continuously with the excitation energy. Accordingly, we consider that the Sm^{2+} ions at different sites have the same type of ligand structures in this sample, and that the inhomogeneous spreads of the energies of the Sm^{2+} ion are due to the continuous site-to-site variation of the crystal-field strength acting on the Sm^{2+} ion.

We notice in Fig. 4 that the highest-energy line among the three shifts remarkably to higher energies with increase of the 7F_0 - 5D_0 excitation energy, while the energies of the other two lines are rather insensitive to the excitation energy. Such difference in the behavior of the three 5D_0 - 7F_1 lines is considered to be due to the difference in the symmetries of the wave functions that express the three 7F_1 Stark levels. The result in Fig. 4 is

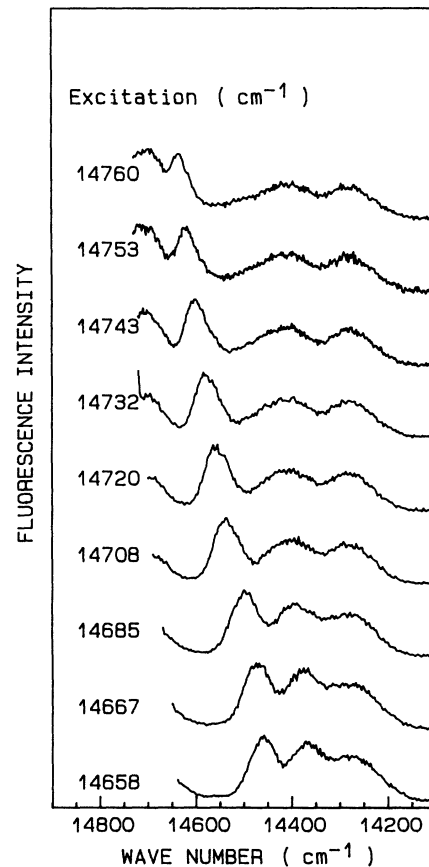


FIG. 3. Fluorescence spectra due to the 5D_0 - 7F_1 transition of Sm^{2+} in fluoride glass at 77 K under dye-laser excitation into the inhomogeneously broadened 7F_0 - 5D_0 absorption line. The fluorescence intensity is normalized to the peak value of the highest-energy component of the three lines due to the 5D_0 - 7F_1 transition.

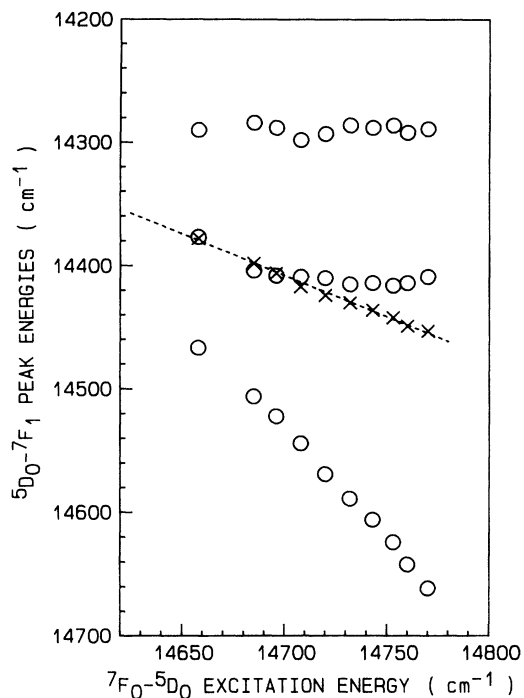


FIG. 4. Peak energies (\circ) and mean energy (\times) of the three fluorescence lines due to the 5D_0 - 7F_1 transition of Sm^{2+} in fluoride glass at 77 K as a function of the 7F_0 - 5D_0 excitation energy. The dashed straight line is fitted for the mean energy by the least-squares method, and has a slope of 0.67. The linear correlation coefficient is 1.00 for this fitting.

similar to that for the Eu^{3+} ion in oxide glasses,^{7,16,18} although it is much different from that for the Eu^{3+} in fluoride glass, in which only the lowest-energy component of the three 5D_0 - 7F_1 lines moves toward lower energies while the other lines move toward higher energies with increase of the 5D_0 - 7F_0 energy separation.⁸

Now, we discuss the point symmetry of the Sm^{2+} ion site in the fluoride glass. From the presence of the intense 5D_0 - 7F_J ($J=0,2,4$) fluorescence lines due to the forced electric-dipole transition shown in Fig. 1, it is clear that the Sm^{2+} ion lies at the site without inversion symmetry. Furthermore, since the J degeneracy of the 7F_1 manifold is completely removed, the point symmetry of the Sm^{2+} ion site is restricted to D_2 , C_{2v} , C_2 , C_S , or C_1 . In D_2 symmetry, however, the electric-dipole 5D_0 - 7F_0 transition is forbidden, because the $J=0$ state belongs to the irreducible representation A , while x , y , and z belong to the B_3 , B_2 , and B_1 representations, respectively. Therefore, D_2 symmetry must be excluded. Furthermore, because there is distinction between the symmetries of the three 7F_1 Stark levels, the C_1 symmetry is also excluded. As a result, we can restrict the point symmetry at the Sm^{2+} ion site to C_{2v} , C_2 , or C_S . These symmetries permit the presence of the linear crystal-field component acting on the Sm^{2+} ion.

In the case of these point symmetries, the $M_J=0$ component is assigned to the lowest energy of the 7F_1 Stark levels, on the basis of the above discussion, because only the $M_J=0$ component of the 7F_1 Stark levels has a large

electron distribution along the z axis, while the other two components are in the x - y plane. Then, we can estimate the values of the second-order crystal-field parameters B_{20} and $|B_{22}|$ for the sites selected by the 7F_0 - 5D_0 excitation from the energies of the three 5D_0 - 7F_1 fluorescence lines in Fig. 4.^{16,18} Figure 5 shows the second-order crystal-field parameters plotted as a function of the 7F_0 - 5D_0 excitation energy. The value of the axial crystal-field parameter B_{20} varies remarkably with the 7F_0 - 5D_0 excitation energy, while $|B_{22}|$, which indicates the strength of the x - y component of the second-order crystal field, remains almost constant. Such large variation only in B_{20} may justify the above assignment for the $M_J=0$ component of the 7F_1 Stark level, which shifts remarkably with the 7F_0 - 5D_0 excitation energy in Fig. 4.

D. FLN experiment under 7F_0 - 5D_1 excitation

Figure 6 shows the FLN spectra due to the 5D_0 - 7F_0 transition at 77 K for the 7F_0 - 5D_1 excitation. The excitation source was the same as that for the 7F_0 - 5D_0 excitation. A hole is also known to be burnable in the 7F_0 - 5D_1 absorption line,²⁵ so that we again took care not to burn a hole in the FLN measurement. In the upper three spectra of Fig. 6, four lines are observed in the energy region of the 5D_0 - 7F_0 transition. The lowest-energy one of these lines is broader than the other three lines (denoted by arrows) and its energy position is fixed at about 14700 cm^{-1} even if the excitation energy is varied. This line is considered to be again due to the excitation-migration effect for the same reasons as noted above. The other three lines shift to lower energies with decrease of the excitation energy, which is also observed for the three lines in the lower three spectra of Fig. 6. The observation of

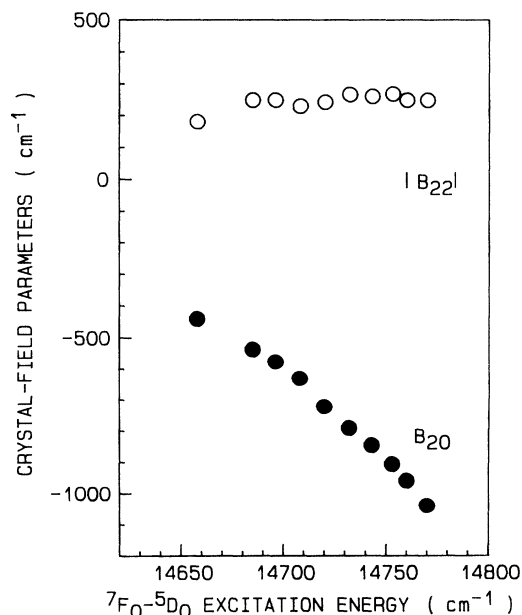


FIG. 5. Second-order crystal-field parameters for Sm^{2+} in fluoride glass versus the 7F_0 - 5D_0 excitation energy.

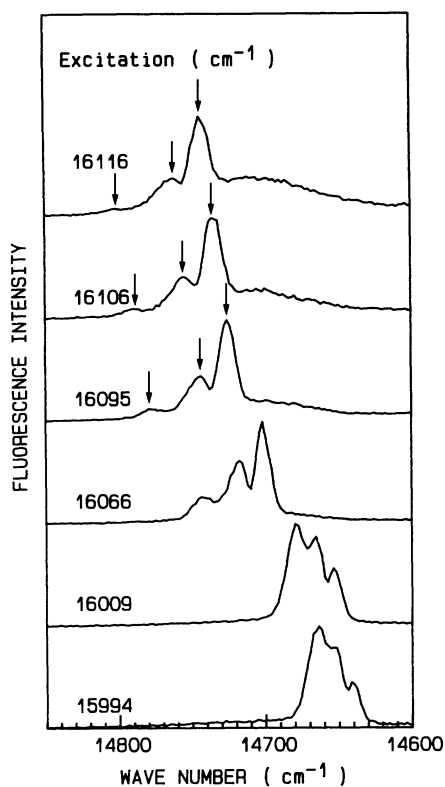


FIG. 6. Fluorescence spectra due to the 5D_0 - 7F_0 transition of Sm^{2+} in fluoride glass at 77 K under dye-laser excitation into the inhomogeneously broadened 7F_0 - 5D_1 absorption line. In the upper three spectra, the arrows denote the 5D_0 - 7F_0 fluorescence lines of Sm^{2+} ions at three different sites.

three similar lines was also reported in Eu^{3+} -doped oxide glasses and they were assigned to the 5D_0 - 7F_0 lines of Eu^{3+} ions in three different sites for which the exciting photon energy is resonant with the 7F_0 - 5D_1 energy separation.^{10,16} The same assignment is considered to be effective also for our sample. Thus, it is possible to determine the energies of the Stark levels of the 5D_1 manifold from analysis of Fig. 6.

Figure 7 shows the energies of the three 5D_1 Stark levels measured from the 5D_0 state as a function of the peak energy of the 5D_0 - 7F_0 fluorescence line. The splitting pattern of the 5D_1 manifold is similar to that of the 7F_1 manifold, but the site-to-site variations of the energies of the 5D_1 Stark levels are much smaller than those of the 7F_1 levels. This is the same result as those for Eu^{3+} in lithium borate¹⁰ and calcium metaphosphate glasses.^{15,16} When the J mixing for the Stark levels of the above two

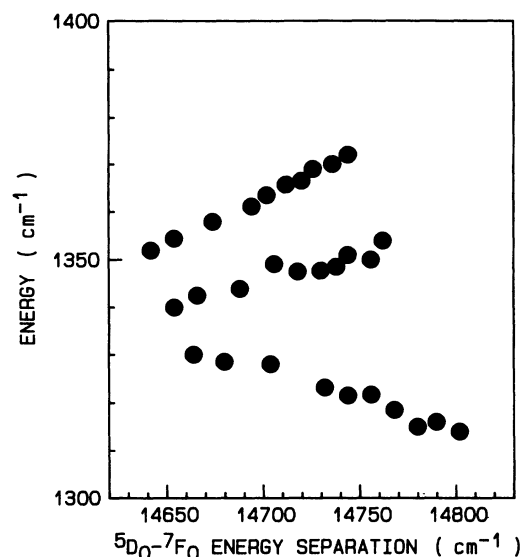


FIG. 7. Energies of the 5D_1 Stark levels of the Sm^{2+} ion in fluoride glass as a function of the 5D_0 - 7F_0 energy separation. The energy of the 5D_0 level was employed as the origin.

manifolds is not taken into account, the ratio of the splitting of the 5D_1 state to that of the 7F_1 state is roughly estimated as 0.28, by employing the free-ion wave functions of the Sm^{2+} ion in the intermediate coupling scheme calculated by Ofelt.²⁶ Experimentally, the above ratio is about 0.15. This difference is considered to result from neglect of the J mixing. This effect is much more important for the 7F_1 state than for the 5D_1 state for the following two reasons. First, the energy separations between the 7F_J states are much smaller than those between the 5D_J states. Second, the absolute value of the reduced matrix element $\langle f^6 {}^7F \| U^{(2)} \| f^6 {}^7F \rangle$ is larger than that of $\langle f^6 {}^5D \| U^{(2)} \| f^6 {}^5D \rangle$. The second reason also accounts for the large difference between the 7F_1 and 5D_1 manifolds in the splitting interval mentioned above. In the Eu^{3+} ion in lithium borate and calcium metaphosphate glasses, the above ratio of the splitting was found to be about 0.2.^{10,15,16} This value is closer to the ratio estimated above. This is probably due to the fact that the energy separations between the 7F_J states are larger in the Eu^{3+} -doped materials than in the Sm^{2+} -doped ones, as shown in Table II. Accordingly, the contribution of the J -mixing effect to the 7F_1 state is small in the above Eu^{3+} -doped glasses, compared with that in the Sm^{2+} -doped fluoride glass.

Next, we focus our attention on the mean energy of the three Stark levels of the 7F_1 manifold. As shown in Fig.

TABLE II. Mean energies of the 7F_J ($J=0,2,3,4$) manifolds relative to that of the 7F_1 manifold in Sm^{2+} -doped fluoride glass and Eu^{3+} -doped oxide glasses. Units are cm^{-1} .

	7F_0	7F_1	7F_2	7F_3	7F_4
Fluoride glass: Sm^{2+}	~ -295	0	~ 560	~ 1250	~ 1990
$\text{Ca}(\text{PO}_3)_2:\text{Eu}^{3+}$ (24 mole %)	~ -375	0	~ 680	~ 1750	~ 2530
$80\text{GeO}_2 \cdot 20\text{Na}_2\text{O} \cdot 1\text{Eu}_2\text{O}_3$	~ -395	0	~ 650	~ 1620	~ 2480
$70\text{SiO}_2 \cdot 30\text{Na}_2\text{O} \cdot 1\text{Eu}_2\text{O}_3$	~ -385	0	~ 660	~ 1730	~ 2570

4, this energy varies with the 5D_0 - 7F_0 energy separation. This result cannot be explained without the J -mixing effect for the 7F_1 state, because the mean energy of the 7F_1 Stark is independent of the crystal-field strength, when we consider only mixing within the 7F_1 manifold.^{15,16,18} If we take into account the J mixing for the 7F_0 and 7F_1 states by the second-order crystal-field potential, the mean energy of the three 7F_1 Stark levels is predicted to be linearly correlated with the energy separation between the 5D_0 and 7F_0 states.^{16,18} In practice, the mean energy of the 5D_0 - 7F_1 fluorescence lines increases linearly with a slope of 0.67 with increase of the 5D_0 - 7F_0 energy separation, as shown in Fig. 4. This slope agrees fairly well with the theoretical value:

$$\frac{\Delta_{20}}{8} \left[\frac{4}{\Delta_{31}} + \frac{1}{\Delta_{21}} \right] = 0.53 . \quad (6)$$

Here, $\Delta_{JJ'}$ is the energy separation between the 7F_J and ${}^7F_{J'}$ states in the free-ion state. In the above calculation, we have put $\Delta_{20}=808$, $\Delta_{21}=517$, and $\Delta_{31}=1190$ cm^{-1} , which values are obtained from the free-ion energy-level scheme of the Sm^{2+} ion calculated by Ofelt.²⁶ Such a good agreement suggests that the inhomogeneous distributions of the energy of the 7F_0 state and the mean energy of the 7F_1 Stark levels are due to the site-to-site variation of the second-order components of the crystal-field potential. The slight difference between the calculated and measured values of the slope may be ascribed to neglect of the J -mixing effect due to the fourth- and sixth-order crystal-field components.

Since the slope of the mean energy of the 5D_0 - 7F_1 fluorescence lines in Fig. 4 is nearly equal to those in Eu^{3+} -doped oxide glasses,^{16,18} we cannot find the effect of the fairly low $4f^55d$ energies on the 7F_1 state through the odd-parity crystal-field potential in our sample. Further,

as discussed above, the site-to-site variations in the energies of the 5D_1 , 5D_0 , 7F_1 , and 7F_0 states of the Sm^{2+} ion in fluoride glass appear to be explained well only by a mixture of the $4f^6$ electron configuration states through the even-parity components of the crystal-field potential. This situation is very similar to those in the Eu^{3+} -doped oxide glasses. However, the 5D_0 - 7F_0 transition mechanism of the Sm^{2+} ion in fluoride glass is due to a mixture of the $4f^55d$ states into the $4f^6$ states through the linear term of the crystal-field potential, as mentioned before. This is in contrast with Eu^{3+} in oxide glasses, in which the intensity of the same line can be explained by the J -mixing effect.¹⁵⁻¹⁸

Finally, the 7F_0 - 5D_0 excitation-energy dependence of the energies of the three 5D_0 - 7F_1 fluorescence lines in our sample is very similar qualitatively to that observed for the Eu^{3+} ion in oxide glasses rather than to that for the Eu^{3+} ion in fluoride glass. This shows that there is a possibility that Sm^{2+} in fluoride glass and Eu^{3+} in oxide glasses resemble each other in the local structure around the rare-earth ions, and also that the geometric model for the first coordination sphere of the Eu^{3+} ion in oxide glasses proposed by Brecher and Riseberg^{7,8} may be applicable to the Sm^{2+} ion in fluoride glass.

ACKNOWLEDGMENTS

The authors are indebted to Dr. T. Izumitani and Mr. M. Matsukawa of Hoya Corporation for providing the samples used in this work. The Eu^{3+} -doped calcium metaphosphate glass and germanate and silicate glasses used in the determination of the values in Tables I and II were supplied by Professor E. Takushi of University of the Ryukyus and Dr. S. Todoroki of NTT Corporation, respectively. The authors also thank Dr. A. Kurita for stimulating discussions.

¹M. M. Weber, in *Laser Spectroscopy of Solids*, edited by W. M. Yen and P. M. Selzer, Topics in Applied Physics Vol. 49 (Springer-Verlag, Berlin, 1981), p. 189.

²A. Szabo, Phys. Rev. Lett. **25**, 924 (1970); **27**, 323 (1971).

³L. A. Riseberg, Phys. Rev. Lett. **28**, 786 (1972); Solid State Commun. **11**, 469 (1972); Phys. Rev. A **7**, 671 (1973).

⁴N. Motegi and S. Shinoya, J. Lumin. **8**, 1 (1973).

⁵T. Kushida and E. Takushi, Phys. Rev. B **12**, 824 (1975).

⁶P. M. Selzer, D. L. Huber, D. S. Hamilton, W. M. Yen, and M. J. Weber, Phys. Rev. Lett. **36**, 813 (1976).

⁷C. Brecher and L. A. Riseberg, Phys. Rev. B **13**, 81 (1976).

⁸C. Brecher and L. A. Riseberg, Phys. Rev. B **21**, 2607 (1980).

⁹O. K. Alimov, T. T. Basiev, Yu. K. Voron'ko, L. S. Gaïgerova, and A. V. Dmitryuk, Sov. Phys. JETP **45**, 690 (1977).

¹⁰J. Hegarty, W. M. Yen, and M. J. Weber, Phys. Rev. B **18**, 5816 (1978).

¹¹T. T. Basiev, M. A. Borik, Yu. K. Voron'ko, V. V. Osiko, and V. S. Fedorov, Opt. Spectros. (USSR) **46**, 510 (1979).

¹²S. A. Brawer and M. J. Weber, Phys. Rev. Lett. **45**, 460 (1980).

¹³M. J. Weber and S. A. Brawer, J. Phys. (Paris) Colloq. **43**, 291 (1982).

¹⁴F. J. Bergin, J. F. Donegan, T. J. Glynn, and G. F. Imbusch, J. Lumin. **34**, 307 (1986).

¹⁵G. Nishimura and T. Kushida, Phys. Rev. B **37**, 9075 (1988).

¹⁶G. Nishimura and T. Kushida, J. Phys. Soc. Jpn. **60**, 683 (1991); **60**, 695 (1991).

¹⁷G. Nishimura, M. Tanaka, A. Kurita, and T. Kushida, J. Lumin. **48/49**, 473 (1991).

¹⁸M. Tanaka, G. Nishimura, and T. Kushida (unpublished).

¹⁹R. I. Personov, in *Spectroscopy and Excitation Dynamics of Condensed Molecular Systems*, edited by V. M. Argranovich and R. M. Hochstrasser (North-Holland, Amsterdam, 1983), p. 555.

²⁰J. S. Ahn, Y. Kanematsu, and T. Kushida, J. Lumin. **48/49**, 405 (1991); Phys. Rev. B **48**, 9058 (1993).

²¹Y. Kanematsu, J. S. Ahn, and T. Kushida, J. Lumin. **53**, 235 (1992); Phys. Rev. B, **48**, 9066 (1993).

²²R. Jaaniso and H. Bill, Europhys. Lett. **16**, 569 (1991).

²³K. Holliday, C. Wei, M. Croci, and U. P. Wild, J. Lumin. **53**, 227 (1992).

²⁴A. Kurita, T. Kushida, T. Izumitani, and M. Matsukawa, in *Spectral Hole-Burning and Luminescence Line-Narrowing, Science and Applications*, (Optical Society of America, Washington, DC, 1992), Vol. 22, p. 163.

²⁵A. Kurita, T. Kushida, T. Izumitani, and M. Matsukawa (unpublished).

- ²⁶G. S. Ofelt, *J. Chem. Phys.* **38**, 2171 (1963).
- ²⁷T. Izumitani and S. A. Payne, *J. Lumin.* **54**, 337 (1993).
- ²⁸A. Kurita (private communication).
- ²⁹K. Hirao, S. Todoroki, and N. Soga, *J. Non-Cryst. Solids* **143**, 40 (1992).
- ³⁰L. A. Riseberg and H. W. Moos, *Phys. Rev. Lett.* **19**, 1423 (1967).
- ³¹H. W. Moos, *J. Lumin.* **1/2**, 106 (1970).
- ³²M. J. Weber, *Phys. Rev. B* **8**, 54 (1973).
- ³³See, for example, L. L. Chase, S. A. Payne, and G. D. Wilke, *J. Phys. C* **20**, 953 (1987).
- ³⁴B. R. Judd, *Phys. Rev.* **127**, 750 (1962).
- ³⁵G. S. Ofelt, *J. Chem. Phys.* **37**, 511 (1962).
- ³⁶B. G. Wybourne, in *Optical Properties of Ions in Crystals*, edited by H. M. Crosswhite and H. W. Moos (Interscience, New York, 1967), p. 35.
- ³⁷M. C. Downer, G. W. Burdick, and D. K. Sardar, *J. Chem. Phys.* **89**, 1787 (1988).
- ³⁸G. W. Burdick, M. C. Downer, and D. K. Sardar, *J. Chem. Phys.* **91**, 1511 (1989).
- ³⁹W. C. Nieuwpoort, G. Blasse, and A. Bril, in *Optical Properties of Ions in Crystals*, edited by H. M. Crosswhite and H. W. Moos (Interscience, New York, 1967), p. 161.
- ⁴⁰C. K. Jørgensen, R. Pappalardo, and E. Rittershans, *Z. Naturforsch. Teil A.* **20**, 54 (1964).
- ⁴¹G. Blasse and A. Bril, *Philips Res. Rep.* **22**, 481 (1967); *J. Chem. Phys.* **50**, 2974 (1969).
- ⁴²R. Reisfeld, *Struct. Bonding (Berlin)* **22**, 123 (1975).